

# Spin Correlations and Magnetic Order in Nonsuperconducting $\text{Nd}_{2-x}\text{Ce}_x\text{CuO}_4$

P.K. Mang<sup>1</sup>, O.P. Vajk<sup>2</sup>, A. Arvanitaki<sup>2</sup>, J.W. Lynn<sup>3</sup>, and M. Greven<sup>1,4</sup>

<sup>1</sup>*Department of Applied Physics, Stanford University, Stanford, CA 94305*

<sup>2</sup>*Department of Physics, Stanford University, Stanford, CA 94305*

<sup>3</sup>*NIST Center for Neutron Research, National Institute for Standards and Technology, Gaithersburg, Maryland 20899 and*

<sup>4</sup>*Stanford Synchrotron Radiation Laboratory, Stanford, CA 94309*

(Dated: February 7, 2020)

We report quantitative neutron scattering measurements of the evolution with doping of the antiferromagnetic correlations, the Néel temperature, and the ordered moment of non-superconducting  $\text{Nd}_{2-x}\text{Ce}_x\text{CuO}_4$  ( $0 \leq x \leq 0.18$ ). The instantaneous correlation length is well described by our quantum Monte-Carlo calculations for the randomly site-diluted nearest-neighbor  $S = 1/2$  square-lattice Heisenberg antiferromagnet. However, the itineracy of the charge carriers results in a relatively strong doping dependence of the ordered moment, consistent with recent theory for the one-band Hubbard model and indicative of a possible quantum critical point well below the geometric site percolation threshold.

PACS numbers: 74.25.Ha, 75.40.Mg, 75.50.Ee

Over the past sixteen years much has been learned about the evolution with doping of magnetic correlations in the high-temperature superconductors. For the prototypical material  $\text{La}_{2-x}\text{Sr}_x\text{CuO}_4$  (LSCO), neutron scattering has led to the observation of the frustration-induced loss of long-range antiferromagnetic order and the concomitant decrease of two-dimensional (2D) spin correlations [1], an incommensurate spin-density wave [2], and coupled charge and magnetic “stripe” order upon co-doping with Nd [3]. To a lesser extent, the existence of interesting magnetic phenomena has also been established in other hole-doped compounds [4]. The richness of the observed behavior is attributable to the evolution of the cuprate superconductors from Mott-insulating parent materials which are found to be excellent realizations (at low energies and long wavelengths) of the spin-1/2 square-lattice Heisenberg antiferromagnet (SLHAF) [5]. Although the vast majority of research has focused on the hole-doped systems, the electron-doped materials, typified by  $\text{Nd}_{2-x}\text{Ce}_x\text{CuO}_{4\pm\delta}$  (NCCO) [6], have presented an important challenge to the field of high- $T_c$  research and particularly to the paradigm established from experiments on LSCO. Unlike LSCO, the magnetic phase of NCCO is very robust with respect to doping [7, 8], the magnetic correlations remain commensurate [8, 9], and there appears to be a first-order transition between the antiferromagnetic and superconducting phases [10].

A related challenge in condensed matter physics lies in the classification and study of strongly correlated electron materials in the vicinity of a quantum critical point (QCP), and the influence of disorder in such systems. As-grown, oxygenated NCCO is not superconducting, and a relatively severe oxygen reduction procedure must be applied to induce superconductivity above  $x = 0.13$  [6]. The occurrence of superconductivity can not be explained on the basis of a reduction-induced change in carrier concentration. It is believed that as-grown samples contain oxygen impurities on the nominally vacant

apical sites [11]. A charge-order instability due to this disorder has been proposed to be related to the lack of superconductivity and the observation of an anomalous pseudogap in the optical conductivity [12]. Furthermore, similar to reports for hole-doped materials, there also exists evidence from transport and tunneling experiments for a QCP in superconducting samples as a function of Ce concentration [13]. While the understanding of quantum phase transitions in the charge-carrier-doped cuprates is still in its infancy, new, quantitative insights have been gained recently into the role of static quantum impurities introduced into the SLHAF [14, 15, 16, 17]. Specifically, it has been found that  $\text{La}_2\text{Cu}_{1-z}(\text{Zn},\text{Mg})_z\text{O}_4$  (LCZMO) is an excellent model system for random site dilution in the quantum-spin limit of spin-1/2 [16], and that the intermediate-temperature properties of this material near the percolation threshold ( $\approx 41\%$  dilution) are influenced by the proximity to a QCP in the extended quantum fluctuation vs. quenched disorder phase diagram [17].

Since superconductivity in the high- $T_c$  cuprates appears in close proximity to antiferromagnetic phases, it is essential to understand the nature of nearby magnetic ground states. In this Letter, we present quantitative neutron scattering results on the evolution with Ce doping of the magnetic properties of as-grown, non-superconducting  $\text{Nd}_{2-x}\text{Ce}_x\text{CuO}_4$  ( $0 \leq x \leq 0.18$ ). We find that the instantaneous spin correlations in the paramagnetic phase are well described by the randomly-diluted spin-1/2 SLHAF model for which we have carried out numerical simulations. As for LCZMO, the Néel temperature of as-grown NCCO corresponds to a contour of constant correlation length of the SLHAF. These observations establish that NCCO, at least when viewed instantaneously in the paramagnetic phase, is, in effect, nearly as good a model system as randomly diluted  $\text{La}_2\text{CuO}_4$  [16]. However, the ordered moment falls off more rapidly, indicating that the dynamics of the itinerant carriers significantly modifies the static magnetic

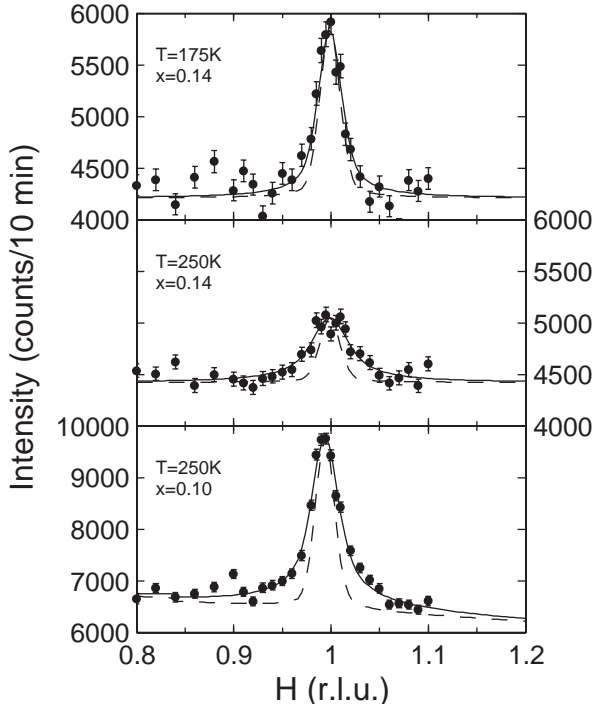


FIG. 1: Representative two-axis scans along  $\mathbf{q}_{2D} = (H/2 - 1/2, H/2 - 1/2)$  in the paramagnetic phase of  $x = 0.10$  and  $0.14$ , with collimations  $40^\circ$ - $42.5^\circ$ -Sample-23.7' and incident neutron energy  $E_i = 14.7$  meV. The instrumental resolution is indicated by the dashed lines.

properties. These data, together with results for the ordered moment of oxygen-reduced (non-superconducting) samples, are consistent with the existence of a QCP well below the nearest-neighbor site-percolation threshold. Finally, we find that up to  $x = 0.10$ , the moment of reduced NCCO is in good agreement with recent theory based on the one-band Hubbard model [18].

Crystals of  $\text{Nd}_{2-x}\text{Ce}_x\text{CuO}_{4\pm\delta}$  were grown in 4 atm of  $\text{O}_2$  using the travelling-solvent floating-zone technique. The solubility limit is just above  $x = 0.18$ , and our study spans the range  $0 \leq x \leq 0.18$ . In addition, two samples ( $x = 0.10$  and  $0.18$ ) were reduced for 20 h at  $920^\circ\text{C}$  in Ar followed by an anneal for 20 h at  $500^\circ\text{C}$  in  $\text{O}_2$ . Our single-grain crystals are cylindrical, typically with a diameter of 4.5 mm, and range in volume from 0.1 to  $0.7 \text{ cm}^3$ . Average Ce concentrations were verified using inductively coupled plasma spectroscopy and found to equal the nominal values. The neutron scattering measurements were performed on the thermal triple-axis instruments BT2 and BT9 of the NIST Center for Neutron Research.

All as-grown samples exhibit long-range magnetic order at low temperature. However, significant 2D magnetic correlations are already present well above the Néel temperature [8]. These may be probed through

“two-axis” scans in which one integrates the dynamic structure factor  $S(\mathbf{q}_{2D}, \omega)$  over the limits set by the thermal energy,  $-k_B T$ , and the incident neutron energy,  $E_i$ . If the integration is carried out over the relevant fluctuations one obtains the equal-time structure factor  $S(\mathbf{q}_{2D})$  [5]. In Fig. 1 we present representative scans of this type that show a clear peak in  $S(\mathbf{q}_{2D})$  at the incipient antiferromagnetic ordering wavevector. We fit these data to a 2D Lorentzian,  $S(q_{2D}) = S(0)/(1 + q_{2D}^2 \xi^2)$ , convolved with the experimental resolution. The instantaneous spin-spin correlation length  $\xi$  is inversely proportional to the peak width. As the temperature or the doping level is increased, correlations decrease, which is reflected in a broadening of the observed peaks.

In Fig. 2 we summarize the behavior of  $\xi(T)$  for several Ce concentrations. We overlay the results of quantum Monte Carlo simulations of the randomly-diluted SLHAF, described by the Hamiltonian

$$\mathcal{H} = J \sum_{\langle i,j \rangle} p_i p_j \mathbf{S}_i \cdot \mathbf{S}_j, \quad (1)$$

where the sum is over nearest-neighbor (NN) sites,  $J$  is the antiferromagnetic Cu-O-Cu superexchange,  $\mathbf{S}_i$  is the spin-1/2 operator at site  $i$ ,  $p_i = 1$  on magnetic sites, and  $p_i = 0$  on nonmagnetic sites. The numerical method is the same as that employed previously [16]. The data are plotted as  $\xi/a$ , the ratio of the spin-spin correlation length to the NN Cu-Cu distance ( $a \approx 3.95 \text{ \AA}$ ), versus  $J/T$ , the ratio of the NN antiferromagnetic superexchange of  $\text{Nd}_2\text{CuO}_4$  to the temperature. A previous estimate from comparison of  $\xi(T)$  with theory for the SLHAF yielded  $J \approx 130$  meV [19], and we find  $J = 125(4)$  meV from comparison with our numerical results for  $x = 0$ . Over a wide temperature range, the spin correlations exhibit an exponential dependence on inverse temperature,  $\xi(x, T) \sim \exp(2\pi\rho_s(x)/T)$ , where  $\rho_s$  is the spin stiffness [8, 16, 20]. With minor adjustments of the effective doping level, presumably due to variations with doping of additional frustrating magnetic interactions and the uncertainty in the oxygen concentration, the experimental data are described excellently by the simulations. We find that  $x_{\text{eff}}(x = 0.10) = 0.08(1)$ ,  $x_{\text{eff}}(x = 0.14) = 0.12(1)$ , and  $x_{\text{eff}}(x = 0.18) = 0.21(2)$ . Also shown are previous data for as-grown samples with  $x = 0$  and  $x = 0.15$  [8]. The result for  $\text{Nd}_2\text{CuO}_4$  agrees well with ours, and we estimate that  $x_{\text{eff}}(x = 0.15) = 0.16(2)$ .

The spin stiffness of the disorder-free spin-1/2 NN SLHAF is known very accurately to be  $2\pi\rho_s/J = 1.131(3)$  [21]. An estimate for the case of quenched disorder, Eq. (1), has been obtained in previous numerical work [16]. Comparison of the experimental results in Fig. 2 gives the effective values  $2\pi\rho_s/J = 0.71(2)$ ,  $0.54(4)$ ,  $0.40(7)$ , and  $0.25(5)$ , respectively, for  $x_{\text{eff}} = 0.08(1)$ ,  $0.12(1)$ ,  $0.16(2)$ , and  $0.21(2)$ . The value  $0.40(7)$  for the  $x = 0.15$  sample is somewhat smaller than the original estimate of

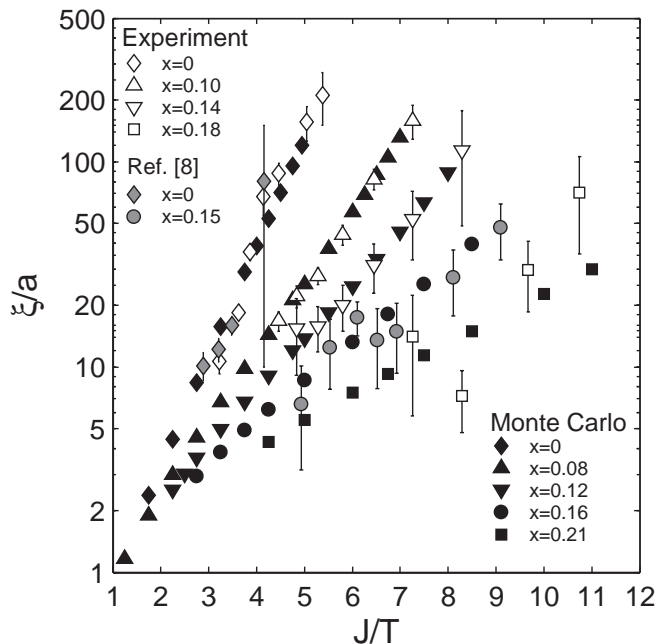


FIG. 2: Semi-log plot of the magnetic correlation length (in units of the lattice constant  $a$ ) versus inverse temperature (in units of  $J = 125$  meV) for  $x = 0, 0.10, 0.14$ , and  $0.18$ . The data are cut off just above the onset of Néel order. Also shown are previous results for  $x = 0$  and  $x = 0.15$  [8]. Quantum Monte-Carlo results for Eq. (1) are shown for comparison.

$2\pi\rho_s/J \approx 0.54$  [8] which was based on a classical rather than a quantum picture [16] for the doping dependence of the spin stiffness.

Figure 3(a) shows that  $T_N(x)$  of our as-grown samples, as obtained from neutron diffraction, approximately follows a parabolic form, extrapolating to zero at  $x \approx 0.22$ . This is consistent with theoretical predictions of the destruction of magnetism in the range  $x = 0.20$  to  $0.25$  [18, 22]. Qualitatively similar behavior has previously been found for reduced NCCO for which  $T_N(x)$  is lower and the antiferromagnetic phase boundary terminates at  $x \approx 0.17$  [7, 23].

The open circles in Fig. 3(a) indicate  $T_N$  for the as-grown samples shown in Fig. 2, but shifted to the effective doping level. For LCZMO it was found that  $T_N(x)$  corresponds well to the contour of constant 2D correlation length  $\xi/a = 100$  as determined numerically for Eq. (1). The solid line in Fig. 3(a) demonstrates that this observation, with  $\xi/a \approx 200$ , also holds for our as-grown crystals of NCCO once the effective doping level is considered. Néel order in  $\text{Nd}_2\text{CuO}_4$  can be estimated to occur when  $(\xi/a)^2 J_{XY}/J \sim 1$ , where  $|J_{XY}/J| \approx 5 \times 10^{-4}$  is the XY anisotropy [1, 5], which is in qualitative agreement with our observations.

We note that Ref. [8] reports data for two as-grown  $x = 0.15$  samples with onset of magnetic order at  $T_N = 160$  and  $125$  K. If we allow for a distribution of Néel

temperatures to account for the rounding of the observed transition, we estimate mean values of  $T_N = 147(17)$  and  $115(9)$  K, respectively. This is consistent with how we have treated our own data. The removal of apical oxygens upon reduction changes both the carrier concentration in the  $\text{CuO}_2$  sheets and the degree of disorder, leading to lower values of  $T_N$ , and to bulk superconductivity as well as a sharp decrease in the antiferromagnetic volume fraction for  $x > 0.13$  [10]. Growth at lower oxygen partial pressure results in crystals with lower oxygen content. The second sample from Ref. [8] has both a lower  $T_N$  and  $\xi(T)$  (not shown in Fig. 2), comparable to our  $x = 0.18$  crystal, leading us to conclude that this sample has a lower oxygen content. In our systematic study of as-grown NCCO we were careful to grow samples under high oxygen partial pressure, resulting in crystals with  $T_N$  at or close to the maximum value attainable.

In Fig. 3(b) we plot the staggered moment, normalized to that of the undoped sample, which we have determined for several Ce concentrations. Consistent with the behavior of  $T_N(x)$ , the staggered moment approaches zero much more rapidly than in the case of quenched disorder where order disappears at the NN square-lattice site percolation threshold. On the other hand, the magnetic phase extends much further than for LSCO [1] and Li-doped  $\text{La}_2\text{CuO}_4$  [26], for which Néel order is destroyed above  $x \approx 0.02$  and  $x \approx 0.03$ , respectively.

As shown in Fig. 3(b), the moment of reduced samples is lowered further and, at least up to  $x = 0.10$ , consistent with a theoretical prediction for the one-band Hubbard model [18]. This theory is based on an analysis of recent ARPES results for the evolution of the Fermi surface of reduced  $\text{Nd}_{2-x}\text{Ce}_x\text{CuO}_{4\pm\delta}$  ( $0 \leq x \leq 0.15$ ) [27], and it argues in favor of a decrease of the effective on-site Coulomb repulsion  $U$  with doping and the concomitant termination of the Néel phase in a QCP. We note that above  $x = 0.13$  the antiferromagnetic (superconducting) volume fraction decreases (increases) sharply [10] and that the treatment of Ref. [18] does not include superconducting fluctuations [25]. Nevertheless, the good agreement up to  $x = 0.10$  appears to support the assertion [18] that  $t - J$  models are intrinsically limited in describing the electron-doped cuprates and that a proper description requires  $t - U$  models with a decreasing value of the repulsion  $U$  with increasing electron concentration.

In the hole-doped compounds the charge carriers have primarily oxygen  $2p$  character, and a small concentration of holes frustrate the magnetic order. On the other hand, the doped electrons in NCCO are believed to predominantly occupy the Cu  $d_{x^2-y^2}$  states, filling the copper  $d$  shell ( $3d^{10}$ ). A dilution picture has been presented as a qualitative explanation of the extent of the antiferromagnetic phase and the behavior of the spin correlations [7, 8, 19]. Our extensive experimental data, in conjunction with the new numerical results, allow us to test the degree to which this picture is quantitatively correct. If

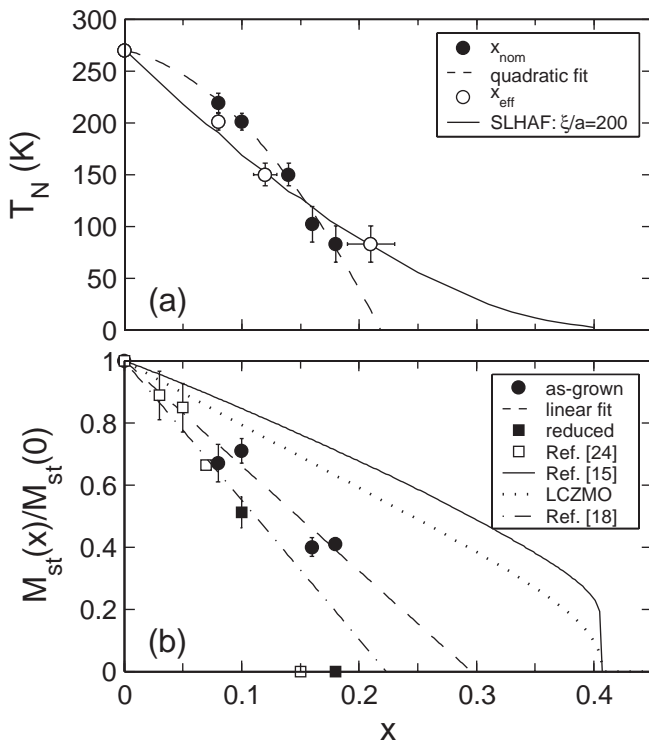


FIG. 3: (a) Doping dependence of the Néel temperature. All Ce-doped samples exhibit some rounding in the transition due to small oxygen and cerium inhomogeneities, which is represented by the vertical error bars; the order parameter data (not shown) were fitted allowing for a Gaussian distribution of Néel temperatures. The dashed curve is a simple quadratic fit to  $T_N(x_{\text{nom}})$  with nominal concentration  $x_{\text{nom}} = x$ . The open symbols indicate  $T_N(x_{\text{eff}})$ , and the continuous line is the contour of  $\xi/a = 200$  obtained from quantum Monte Carlo for Eq. (1). (b) Doping dependence of the ordered copper moment per site, normalized by the value for  $\text{Nd}_2\text{CuO}_4$ . The decrease for as-grown samples is linear up to the highest concentration measured. Also shown are quantum Monte-Carlo results for the diluted SLHAF [15] and data for LCZMO [16]. For reduced samples, the moment falls off more rapidly; the open squares are data obtained in a previous study [24]. The dot-dashed line is a mean-field calculation for NCCO [18, 25].

viewed instantaneously, so as to mitigate the effects due to the increased metallicity upon doping [28], the magnetism of NCCO should indeed resemble a system with quenched random site dilution. What is surprising is the degree to which this correspondence holds *quantitatively*. Yet, since the charge carriers in as-grown NCCO are itinerant even well below  $T_N$ , differences between the two systems can be expected as we view them on different time scales. Indeed, the ordered moment, an indicator of the strength of the magnetic order at infinitely long times, decreases much more rapidly in the case of NCCO than for the SLHAF. Our results point to the existence of a quantum critical point below the geometric site-percolation threshold even in the absence of significant superconducting fluctuations.

We acknowledge valuable discussions with S. Laroche, R.S. Markiewicz, and M. Matsuda, and thank I. Tanaka and the late H. Kojima for their invaluable assistance in the initial stage of the crystal growth effort. This work was supported by the US Department of Energy under Contracts No. DE-FG03-99ER45773 and No. DE-AC03-76SF00515, by NSF CAREER Award No. DMR9985067, and the A.P. Sloan Foundation.

- 
- [1] B. Keimer *et al.*, Phys. Rev. B **46**, 14034 (1992), and references therein.
  - [2] K. Yamada *et al.*, Phys. Rev. B **57**, 6165 (1998), and references therein.
  - [3] J. M. Tranquada *et al.*, Nature (London) **375**, 561 (1995).
  - [4] J. Rossat-Mignod *et al.*, Physica C **185-189**, 86 (1991); H. F. Fong *et al.*, Nature **398** 588 (1999); H. He *et al.*, Science **295**, 1045 (2002).
  - [5] R. J. Birgeneau *et al.*, Phys. Rev. B **59**, 13788 (1999).
  - [6] Y. Tokura, H. Takagi, and S. Uchida, Nature **337**, 345 (1989).
  - [7] G. M. Luke *et al.*, Phys. Rev. B **42**, 7981 (1990).
  - [8] M. Matsuda *et al.*, Phys. Rev. B **45**, 12548 (1992).
  - [9] K. Yamada, K. Kurahashi, Y. Endoh, R. J. Birgeneau, and G. Shirane, J. Phys. Chem. Solids **60**, 1025 (1999).
  - [10] T. Uefuji *et al.*, Physica C **357-360**, 208 (2001).
  - [11] A. J. Schultz *et al.*, Phys. Rev. B **53**, 5157 (1996).
  - [12] Y. Onose *et al.*, Phys. Rev. Lett. **82**, 5120 (1999).
  - [13] P. Fournier *et al.*, Phys. Rev. Lett. **81**, 4720 (1998); L. Alff *et al.*, Nature (London) **422**, 698 (2003).
  - [14] S. Sachdev, C. Buragohain, and M. Vojta, Science **286**, 2479 (1999).
  - [15] A. W. Sandvik, Phys. Rev. B **66**, 024418 (2002).
  - [16] O. P. Vajk *et al.*, Science **295**, 1691 (2002); O. P. Vajk, M. Greven, P. K. Mang, and J. W. Lynn, Solid State Comm. **126**, 93 (2003).
  - [17] A. W. Sandvik, Phys. Rev. Lett. **89**, 177201 (2002); O. P. Vajk and M. Greven, Phys. Rev. Lett. **89**, 172202 (2002).
  - [18] C. Kusko, R. S. Markiewicz, M. Lindroos, and A. Bansil, Phys. Rev. B **66**, 140513R (2002).
  - [19] T. R. Thurston *et al.*, Phys. Rev. Lett. **65**, 263 (1990).
  - [20] S. Chakravarty, B. I. Halperin, and D. R. Nelson, Phys. Rev. B **39**, 2344 (1989).
  - [21] B. Beard, R. J. Birgeneau, M. Greven, and U.-J. Wiese, Phys. Rev. Lett. **80**, 1742 (1998).
  - [22] M. Sugihara, M. A. Ikeda, and P. Entel, Phys. Rev. B **57**, 11760 (1998).
  - [23] T. Uefuji *et al.*, Physica C **378-381**, 273 (2002).
  - [24] M. Rosseinsky, K. Prassides, and P. Day, Inorg. Chem. **30**, 2680 (1991).
  - [25] Ref. [18] is a mean-field theory. Quantum fluctuations will lower  $M_{\text{st}}(x)$ , but the ratio  $M_{\text{st}}(x)/M_{\text{st}}(0)$  is expected to remain approximately unaltered up to  $x = 0.15$ . The linear behavior above  $x = 0.15$  is to be viewed as an upper bound (R.S. Markiewicz, private communication).
  - [26] T. Sasagawa *et al.*, Phys. Rev. B **66**, 184512 (2002).
  - [27] N. P. Armitage *et al.*, Phys. Rev. Lett. **88**, 257001 (2002).
  - [28] The resistivity at 4.2 K has been reported to be as low as  $\rho \sim 2$  m $\Omega$  cm [12].